RSC Advances

PAPER

View Article Online
View Journal | View Issue

Cite this: *RSC Adv.*, 2014, **4**, 41588

Y-shaped block copolymer (methoxy-poly(ethylene glycol))$_2$-*b*-poly(L-glutamic acid): preparation, self-assembly, and use as drug carriers

Lixin Yang,[a] Xiuli Hu,[a] Weiqi Wang,[ab] Shi Liu,[ab] Tingting Sun,[ab] Yubin Huang,[a] Xiabin Jing[a] and Zhigang Xie*[a]

Received 31st July 2014
Accepted 27th August 2014

DOI: 10.1039/c4ra07890j

www.rsc.org/advances

Y-shaped amphiphilic block copolymers, (methoxy-poly(ethylene glycol))$_2$-*block*-poly(L-glutamic acid) ((mPEG)$_2$-PGA) and its precursor (methoxy-poly(ethylene glycol)$_2$-*block*-poly(γ-benzyl-L-glutamate) ((mPEG)$_2$-PBG), were prepared in three steps: (1) macroinitiator (methoxy-poly(ethylene glycol))$_2$-NH$_2$ ((mPEG)$_2$-NH$_2$) was synthesized by coupling two methoxy-poly(ethylene glycol)s with serinol and diisocyanate. (2) (mPEG)$_2$-PBG was synthesized by ring opening polymerization of γ-benzyl-L-glutamate-*N*-carboxyanhydride initiated with the macroinitiator ((mPEG)$_2$-NH$_2$); (3) the protective benzyl groups in (mPEG)$_2$-PBG were removed to obtain (mPEG)$_2$-PGA. The properties of both (mPEG)$_2$-PBG and (mPEG)$_2$-PGA were characterized by ^{1}H NMR, FT-IR, GPC, and DLS. In aqueous solution (mPEG)$_2$-PBG tends to form more stable micelles compared to linear mPEG-PBG copolymer. The size of (mPEG)$_2$-PBG decreases with increasing length of hydrophobic PBG in (mPEG)$_2$-PBG. Paclitaxel and cisplatin were grafted onto (mPEG)$_2$-PGA to form (mPEG)$_2$-PGA-PTX (MPTX) with a grafting ratio of near 90% and (mPEG)$_2$-PGA-Pt (MPt) conjugates with a loading efficacy of 15% (w/w). MPTX can greatly improve the solubility of PTX. Both conjugates can self-assemble into micelles with a mean diameter of about 50 nm and show enhanced anti-cancer activity against MCF-7, HeLa, and SMMC cell lines. The *in vivo* anticancer evaluation in mice shows MPt showed a desirable antitumor activity and allowed us to deduce the system toxicity. Therefore, both MPTX and MPt have a great potential as a polymer drug in cancer chemotherapy.

Introduction

Poly(ethylene glycol)-containing amphiphilic block copolyesters (PEG-PE), such as copolycarbonate (PEG-PC) and copoly(amino acid) (PEG-PAA) have been synthesized and employed as drug carriers.[1–3] With the use of these polymeric drug carriers, it is possible to effectively prolong the circulation time of clinical anti-cancer drugs, to shield the recognition by immune system, to escape the capture of reticuloendothelial system (RES), and to accumulate at tumor site *via* the enhanced permeability and retention (EPR) effect.[4,5] Among these polymer carriers, linear diblock or triblock copolymers have been extensively investigated and some of them have entered clinical trials and shown encouraging clinical results.[6]

Recently, thanks to the development of synthetic methods, such as atom transfer radical polymerization (ATRP), reversible addition fragmentation chain transfer (RAFT) and "click chemistry" reactions, and so on, miktoarm amphiphilic block copolymers have been designed and synthesized such as mPEG-(PLA)$_n$ (n = 2, 4), mPEG$_2$-PLA$_2$, mPEG$_3$-PLA and mPEG-PCL$_2$.[7–9] Compared to linear counterparts, miktoarm amphiphilic block compolymers always have unique self-assembly abilities, resulting in interesting pharmacologic behaviors because of their unique topological structure. Cinziacarofalo *et al.* prepared three shapes of copolymers of general formula mPEG-(PLA)$_n$ (n = 1, 2 or 4; mPEG: mPEG$_{2k}$ or mPEG$_{5k}$; PLA: atactic or isotactic) to evaluate the architecture and chemical composition effect on the micelles formation and stability. Compared to other copolymers, mPEG$_{2k}$-(PD,LLA)$_2$ was able to form monodispersive and stable micelles.[10] Sun *et al.* investigated the effect of solvent and the relative length of the PBG on the self-assembly of Y-shaped copolymer, poly(L-lactide)$_2$-*b*-poly(γ-benzyl-L-glutamate). At a fixed composition of copolymer, the copolymer formed a transparent gel in toluene, while became homogeneous dispersion containing nano-scale fibrous aggregates in benzyl alcohol.[11]

In the past few decades, linear amphiphilic PEG-PAA copolymers, mostly PEG-*b*-poly(aspartic acid), PEG-*b*-poly(glutamic acid) (PEG-PGA), and PEG-*b*-poly(lysine) (PEG-PLL), have been

[a]*State Key Laboratory of Polymer Physics and Chemistry, Changchun Institute of Applied Chemistry, Chinese Academy of Sciences, Changchun 130022, People's Republic of China. E-mail: xiez@ciac.ac.cn; Fax: +86 431-85262779; Tel: +86 431-85262779*

[b]*Graduate School of Chinese Academy of Sciences, Beijing 100049, People's Republic of China*

successfully used to physically encapsulate or chemically bond anti-cancer drugs, such as cisplatin, oxaliplatin, paclitaxel and doxorubicin, *etc.*[12–14] Compared with other drug carriers, PEG-PAA copolymers have their specific features: (1) many amino acids can be chosen and available easily; (2) several amino acids contain functional groups and special functionalization is not needed; (3) some amino acids can exist in different charge states such as neutral in protected form and positive or negative in deprotected form; (4) amino acids have different isoelectric potentials and their solubility is pH dependent; (5) chiral molecular structure and ordered secondary structures of amino acids are often associated with special aggregation behaviors of them. In short, PEG-PAAs are more versatile than other drug carriers. For this reason, many PAAs and PEG-PAAs have been developed to demonstrate their special aggregates and possible application in drug delivery. Nano PAAs or PEG-PAAs prodrugs such as poly(L-glutamic acid)-paclitaxel, (PGA-PTX, XYOTAX™, CT2103), PEG-polyaspartate-DOX (NK911) and PEG-polyaspartate-PTX (NK105), *etc.*, have been developed and evaluated in preclinical or clinical trials.[15,16] From the above discussion about the effect of the topological structure of miktoarm amphiphilic polymers on the self-assemble behaviors and drug delivery, it can be concluded that the variability of amphiphilic PAA with different topologic structures has an ability of extending the scope of amphiphilic PAA prodrugs. Unfortunately, no reports focus on the preparation of Y-shaped amphiphilic PAA prodrugs having two mPEG arms till now, which is expected to have excellent water solubility, unique self-assembly and pharmaceutical behaviors.

Herein, Y-shaped block copolymers of $(mPEG)_2$-*b*-PBG with a variety of PBG block lengths, their deprotection products $(mPEG)_2$-*b*-PGA, and their conjugates with paclitaxel (PTX) and cisplatin, *i.e.*, $(mPEG)_2$-*b*-PGA-PTX and $(mPEG)_2$-*b*-PGA-Pt were synthesized. The self-assembly behaviors of $(mPEG)_2$-*b*-PBG and $(mPEG)_2$-*b*-PGA-PTX were investigated. The *in vitro* and *in vivo* anti-cancer efficacy of and $(mPEG)_2$-*b*-PGA-cisplatin conjugates was further elucidated.

Experimental section

Materials

Methoxy-poly(ethylene glycol) (mPEG) (Mn = 5 kg mol^{-1}) (from Sigma) was dried by azeotropic distillation with toluene before use. Stannous octoate ($Sn(Oct)_2$) (form Sigma Chemical Co.), di-*tert*-butyl dicarbonate (from J&K Scientific Ltd.), 2-amino-1,3-propanediol (serinol, from J&K Scientific Ltd.) and hexamethylenediisocyanate (HDI, from Aladdin Industrial Co.) were used as received. 1,4-Dioxacyclohexane was dried over CaH_2 and distilled over sodium just before use. γ-Benzyl-L-glutamate-*N*-carboxyanhydride (BLG-NCA) were synthesized according to the ref. 17.

Characterizations

^1H NMR spectra were measured by an AV-400 instrument (Bruker BioSpin GmbH, Rheinstetten, Germany). The number-average molecular weights (Mn) and polydispersity indices (PDI) of the polymers were determined by size exclusion chromatography (SEC), which was performed with a Waters 1525 fitted with two columns (Styragel HT3 and HT4, 7.8 × 300 mm), with THF as mobile phase at a flow rate of 1.0 ml min^{-1} and an operating temperature of 35 °C. PS standards were used for calibration. Fourier transform infrared (FTIR) spectra were recorded on a Bio-Rad Win-IR instrument using potassium bromide (KBr) method. The size of micelles was measured by DLS measurements carried out with a DAMN EOS instrument equipped with a He–Ne laser at the scattering angle fixed at 90°. The micelle solution of about 0.5 mg ml^{-1} in water was filtered through a 0.45 μm of filter membrane before measurement. The morphologies of the nanoparticles were confirmed by using transmission electron microscopy (TEM) measurement on a JEOL JEM-1011 transmission electron microscope with an accelerating voltage of 100 kV. A drop of the nanoparticle solution (1 mg ml^{-1}) was deposited onto a 230-mesh copper grid coated with carbon, and was air-dried at room temperature.

Preparation of 2-(*tert*-butyloxycarbamino)-1,3-propanediol (*N*-Boc-serinol, NBS)

2-(*tert*-Butyloxycarbamino)-1,3-propanediol (*N*-Boc-Serinol) was synthesized according to the ref. 18. Briefly, serinol (2-amino-1,3-propanediol) (9.1 g, 0.1 mol) was dissolved in EtOH (90 ml), and then di-*tert*-butyl dicarbonate (23.9 g, 0.11 mol) was dropped. The solution was stirred for 1 hour at room temperature, and the solvent was removed under reduced pressure. The yellow solid was recrystallized from hexane/EtOAc to give NBS as 17.1 g of white solid (yield: 83%). ^1H NMR (400 MHz, DMSO): δ = 5.25 (1H, N*H*), 3.70–3.79 (5H, m, 2 × CH_2OH and C*H*N), 1.44 (9H, s, 3 × CH_3).

Synthesis of macroinitiator $mPEG_{5k}$-NH_2-$mPEG_{5k}$ ($(mPEG)_2$-NH_2)

Dried $mPEG_{5k}$ (15.0 g, 3 mmol) and HDI (0.53 g, 3.15 mmol) were added into a dried flask, 20 ml 1,4-dioxacyclohexane and 0.1 g $Sn(Oct)_2$ were added. The solution was stirred at 70 °C under nitrogen for 1 hour, and then NBS (0.29 g, 1.5 mmol) was added. The solution was stirred for 2 h and then precipitated in cold ether. The precipitate was collected and dried to obtain 14.5 g white product $(mPEG_{5k})_2$-NHBoc (yield: 91.7%). To a 20 ml solution of $(mPEG_{5k})_2$-NHBoc (10.0 g) in dichloromethane, 20 ml trifluoroacetic acid was added. The solution was stirred in ice bath for 1 h and poured into cold ether. The precipitate was filtered out and dried. The product was dissolved in water and neutralized by saturated aqueous sodium bicarbonate. The pH value of the solution was adjusted to 7–8. The solution was dialyzed against water using a dialysis bag (MWCO 3500 g mol^{-1}) for 2 days and frozen-dried to obtain 8.5 g of white product $(mPEG_{5k})_2$-NH_2 (yield: 85%).

Synthesis of Y-shaped copolymer $mPEG_{5k}$-PBG-$mPEG_{5k}$ ($(mPEG_{5k})_2$-PBG) and linear copolymer $mPEG_{5k}$-PBG

Three kinds of $(mPEG_{5k})_2$-PBG with different PBG lengths, *i.e.*, $(mPEG_{5k})_2$-PBG_{14}, $(mPEG_{5k})_2$-PBG_{20} and $(mPEG_{5k})_2$-PBG_{35}, were prepared by the ROP of BLG-NCA initiated by $(mPEG_{5k})_2$-NH_2. A

typical synthetic procedure for $(mPEG_{5k})_2$-PBG_{20} is as follows: dried $(mPEG_{5k})_2$-NH_2 (3.0 g) as a macroinitiator and BLG-NCA (1.5 g) were dissolved in 5 ml dried DMF. The solution was stirred at 25 °C for 72 h and then precipitated in cold ether. The precipitate was collected and dried to obtain white product $(mPEG_{5k})_2$-PBG_{20}. Linear copolymers $mPEG_{5k}$-PBGs with DP of PBG of 14, 20, and 35, respectively, were prepared by the same way, but with $mPEG_{5k}$-NH_2 as the macroinitiator.

Synthesis of methoxy-poly(ethylene glycols)$_2$-*b*-poly-(L-glutamic acid) ($(mPEG_{5k})_2$-PGA)

$(mPEG_{5k})_2$-PBG (1.5 g) was dissolved in a mixed solution of 6 ml of CF_3COOH and 2 ml of 33 wt% HBr/acetic acid. The solution was stirred at room temperature for 2.5 h and poured into excessive ether. The precipitate was filtered out and dried to obtain white product $(mPEG_{5k})_2$-PGA.

Synthesis of $(mPEG)_2$-PGA-PTX prodrug (MPTX)

To a 20 ml solution of $(mPEG_{5k})_2$-PGA_{35} (200 mg, 0.012 mmol) and PTX (70 mg, 0.08 mmol), DCC (105 mg, 0.51 mmol) and DMAP (30 mg, 0.25 mmol) were added. The solution was stirred at room temperature for 8 h, and then precipitated in a mixture of cold ether–ethanol. The product was collected and dried. PTX content in the prodrug was determined by ^{1}H NMR. The PTX content and its graft efficacy were calculated according to the following formula: PTX (wt%) = (weight of PTX/weight of prodrug) × 100% and PTX graft efficiency (wt%) = (weight of PTX in prodrug/weight of PTX in feed) × 100%, respectively.

Synthsis of $(mPEG)_2$-PGA-cisplatin prodrug (MPt)

Cisplatin (150 mg, 0.5 mmol) was dissolved into 20 ml water, and then $AgNO_3$ (170 mg, 1.0 mmol) was added, the solution was stirred under dark for 24 h. To the clear solution obtained by removal of the white precipitate formed *via* filtration, was added $(mPEG_{5k})_2$-PGA_{35} (300 mg, 0.018 mmol). The solution was stirred under dark for 8 h, and then dialyzed against water using a dialysis bag (MWCO 3500 g mol^{-1}) for 1 day and frozen-dried to obtain 450 mg of white product MPt.

Cell culture

MCF-7, HeLa, and SMMC cell lines were purchased from the Institute of Biochemistry and Cell Biology, Chinese Academy of Sciences, Shanghai, China and were grown in Dulbecco's modified Eagle's medium (DMEM, GIBCO) supplemented with 10% heat-inactivated fetal bovine serum (FBS, GIBCO), 100 U ml^{-1} penicillin, and 100 μg ml^{-1} streptomycin (Sigma), and the culture medium was replaced once very day.

In vitro MTT assay

MCF-7 cells harvested in a logarithmic growth phase were seeded in 96-well plates at a density of 10^5 cells per well and incubated in RPMI 1640 for 24 h. The medium was then replaced by various drug formulations of PTX, $(mPEG_{5k})_2$-PGA_{35} and $(mPEG_{5k})_2$-PGA_{35}-PTX. To test the cytotoxicity of the free drug carrier, just $(mPEG_{5k})_2$-PGA_{35} was used to treat the cells and its amount was equal to that used in $(mPEG_{5k})_2$-PGA_{35}-PTX. All of the drugs with PTX were modulated to a series of final equivalent PTX concentrations ranging from 0.005 to 50 μg ml^{-1}. The incubation of each drug formulation was continued for 48 h or 72 h. Then, 20 μl of MTT solution of 5 mg ml^{-1} in PBS was added and the plates were incubated for another 4 h at 37 °C, followed by removal of the culture medium containing MTT and addition of 150 μl of DMSO to each well to dissolve the formazan crystals formed. Finally, the plates were shaken for 10 minutes, and the absorbance of formazan formed was measured at 492 nm by a microplate reader. The cell viability against HeLa and SMMC lines was determined by the similar way.

In vivo evaluation

Animal model preparation. Chinese Kunming (KM) female mice were obtained from Jilin University, China (56–84 days old, 20–25 g in weight) and maintained under required conditions. All animal studies were conducted in accordance with the principles and procedures outlined in "Regulations for the Administration of Affairs Concerning Laboratory Animals", approved by the National Council of China on October 31, 1988, and "The National Regulation of China for Care and Use of Laboratory Animals", promulgated by the National Science and Technology Commission of China, on November 14, 1988. To develop the tumor xenografts, H22 cells were injected into the lateral aspect of the right anterior limb of the mice (5×10^6 cells in 0.1 ml PBS). After the tumor volume reached 100–200 mm^3, the hair of the mice was removed with a sodium sulfide solution (80 g L^{-1} in 30 vol% aqueous alcohol).

Anti-tumor efficacy. Thirty two KM mice bearing H22 tumor nodules were randomly divided into four groups for (a) normal saline (control); (b) cisplatin, 3 mg Pt per kg; (c) MPt, 3 mg Pt per kg and (d) MPt, 6 mg Pt per kg. Before injection, all the mice were marked and weighed, and the length and width of the tumors were measured as the initial size on day 1. The day of the first injection was designated as day 1. For groups (b) to (d), designed doses of Pt were intravenously injected *via* tail vein on day 1, day 3, and day 5, separately. For group (a), the mice were injected with equivalent volume of normal saline. The tumor size was measured every other day and the tumor volume (V) was calculated by the formula of $V = ab^2/2$, where a and b were the length and width of tumor, respectively.

Statistics. The data were expressed as the mean ± standard deviation (SD). The Student's t-test was used to determine the statistical difference between various experimental and control groups. Differences were considered statistically significant at a level of $p < 0.05$.

Results and discussion

Synthesis of Y shaped amphiphilic copolymers

In order to prepare Y shaped amphphilic block polymer, that is, methoxy-poly(ethylene glycol)$_2$-*block*-poly(γ-benzyl-L-glutamate) ($(mPEG_{5k})_2$-PBG), two main synthetic strategies were adopted. One is that the coupling reaction between isocyanate group and

hydroxyl group is always adopted to prepare copolymers containing accurate structure, such as hydrogels and drug carriers.[19,20] The other is the ring-opening polymerization (ROP) of corresponding amino acid NCA monomers initiated by primary amines. Various poly(ethylene glycol)-containing copolypeptides with well controlled degrees of polymerization (DP) have been synthesized by this way,[21,22] which helps to the preparation of the accurate structure of drug carriers.

In this work, three Y-shaped $(mPEG_{5k})_2$-PBG and $(mPEG_{5k})_2$-PGA copolymers with different PBG or PGA lengths were prepared in three steps as shown in Scheme 1: (1) synthesis of macroinitiator $(mPEG_{5k})_2$-NH_2. Briefly, $mPEG_{5k}$ was reacted with HDI to form $mPEG_{5k}$-NCO, then two $mPEG_{5k}$-NCOs were coupled with NBS to obtain $(mPEG_{5k})_2$-NHBoc, and finally, complete removal of Boc group from $(mPEG_{5k})_2$-NHBoc by HBr/HAc/CF_3COOH to afford $(mPEG_{5k})_2$-NH_2. (2) $(mPEG_{5k})_2$-PBG was synthesized by the ROP of *N*-carboxyanhydride of γ-benzyl-L-glutamate (BLG-NCA) initiated by $(mPEG_{5k})_2$-NH_2. (3) The benzyl groups on the PBG block were removed by HBr/HAc/CF_3COOH to afford $(mPEG_{5k})_2$-PGA.

The structures of $(mPEG_{5k})_2$-NHBoc and $(mPEG_{5k})_2$-NH_2 were confirmed by ^{1}H NMR and FT-IR. The ^{1}H NMR spectra of $(mPEG_{5k})_2$-NHBoc and $(mPEG_{5k})_2$-NH_2 are shown in Fig. 1. As shown in Fig. 1A, peaks a at 3.38 ppm and b at 3.62 ppm are assigned to the protons of CH_3O– and –OCH_2CH_2O– units of mPEG of $(mPEG_{5k})_2$-NHBoc. The peaks marked with c (3.14 ppm), d (1.47 ppm) and e (1.32 ppm) are assigned to the protons of methylene units of HDI. Peak h at 1.42 ppm is assigned to –O–$C(CH_3)_3$ unit in NBS. After the removal of the protecting group (Boc) in $(mPEG_{5k})_2$-NHBoc, peak h at 1.42 ppm disappeared completely in Fig. 1B, indicating successful synthesis of macroinitiator $(mPEG_{5k})_2$-NH_2.

FT-IR spectra of $(mPEG_{5k})_2$-NHBoc and $(mPEG_{5k})_2$-NH_2 are shown in Fig. 2B and C. Compared to that of mPEG5k in Fig. 2A, the peaks at 1721 cm^{-1} (C=O stretching) and 1533 cm^{-1} (amide II mode) in $(mPEG_{5k})_2$-NHBoc appeared and the peak at 3475 cm^{-1} (OH stretching) disappeared, indicating successful synthesis of $(mPEG_{5k})_2$-NHBoc. After the removal of Boc group

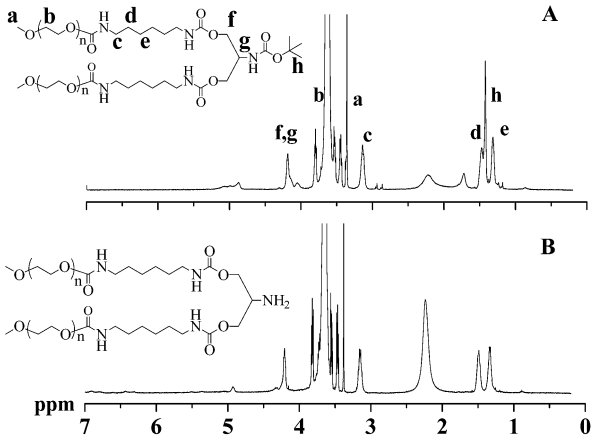

Fig. 1 ^{1}H NMR spectra of $(mPEG_{5k})_2$-NHBoc (A) and $(mPEG_{5k})_2$-NH_2 (B) in $CDCl_3$.

in $(mPEG_{5k})_2$-NHBoc, the peak at 3352 cm^{-1} appeared in Fig. 3C and was assigned to free NH_2 group of $(mPEG_{5k})_2$-NH_2.

The structure of $(mPEG_{5k})_2$-NHBoc can also be proved by GPC. As shown in Fig. 3 and Table 1, $mPEG_{5k}$ and $mPEG_{10k}$ gave GPC peaks at 17.1 and 15.7 min, respectively, while that of $(mPEG_{5k})_2$-NHBoc was at 15.7 min, close to that of $mPEG_{10k}$. This is understandable, because $(mPEG_{5k})_2$-NHBoc is two $(mPEG_{5k})$s coupled with an HDI-seritol-HDI linkage. Of course, the molecular weight values determined by GPC were not exactly 5k or 10k, but their two-fold relationship did exist (8.4 *vs.* 16.4 kg mol^{-1}, Table 1). Moreover, the unimodal peak shape of $(mPEG_{5k})_2$-NHBoc and the narrow distribution (PDI = 1.02) in Fig. 3C also provided evidence for absence of $mPEG_{5k}$ residues and successful synthesis of $(mPEG_{5k})_2$-NHBoc. Additionally, by comparing integral area of peak b (Fig. 1) at 3.62 ppm assigned to the protons of –CH_2CH_2O– units in mPEG with that of peak c at 3.14 ppm assigned to the protons of –NH–$CH_2CH_2CH_2CH_2$-CH_2CH_2–NH– in HDI, no change was found before and after the deprotection (data not shown), indicating that CF_3COOH did not cause chain cleavage of $(mPEG_{5k})_2$-NHBoc during its deprotection. In a word, well defined $(mPEG_{5k})_2$-NH_2 was

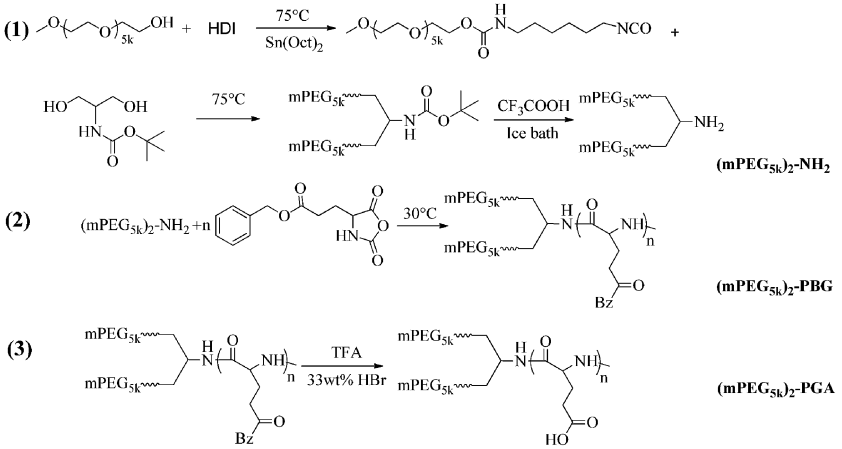

Scheme 1 Synthetic routes of $(mPEG_{5k})_2$-NH_2, $(mPEG_{5k})_2$-PBG and $(mPEG_{5k})_2$-PGA.

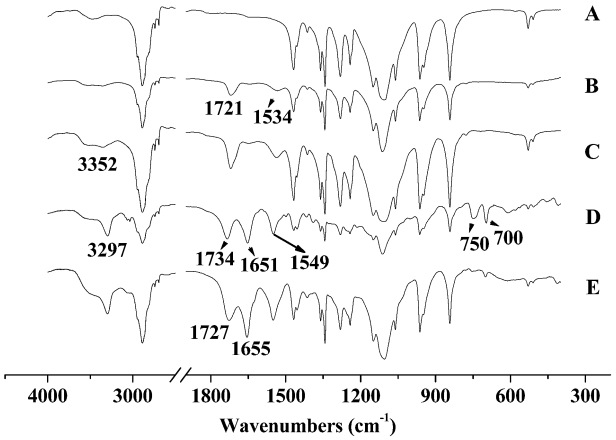

Fig. 2 FT-IR spectra of $mPEG_{5k}$ (A), $(mPEG_{5k})_2$-NHBoc (B), $(mPEG_{5k})_2$-NH_2 (C), $(mPEG_{5k})_2$-PBG_{35} (D), and $(mPEG_{5k})_2$-PGA_{35} (E).

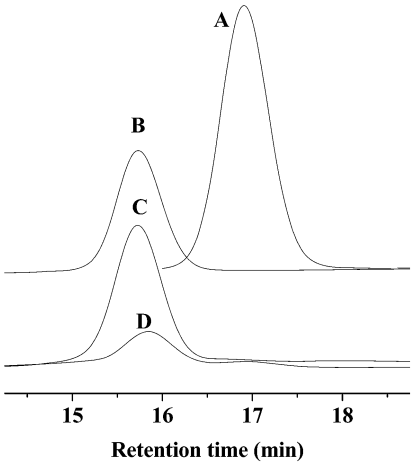

Fig. 3 The GPC traces of $mPEG_{5k}$ (A), PEG_{10k} (B), $(mPEG_{5k})_2$-NHBoc (C) and $(mPEG_{5k})_2$-PBG_{20} (D).

Table 1 GPC results of $mPEG_{5k}$, PEG_{10k}, $(mPEG_{5k})_2$-NHBoc, $mPEG_{5k}$-PBGs and $(mPEG_{5k})_2$-PBGs

Samples	Mn (kg mol^{-1})	PDI	Mn[a] (kg mol^{-1})	DP[b]
$mPEG_{5k}$	8.44	1.02	5.0	
$mPEG_{10k}$	16.2	1.02	10.0	
$(mPEG_{5k})_2$-NHBoc	16.4	1.02	10.0	
$(mPEG_{5k})_2$-PBG_{14}	14.8	1.03	11.7	13/12
$(mPEG_{5k})_2$-PBG_{20}	12.7	1.08	12.5	19/19
$(mPEG_{5k})_2$-PBG_{35}	15.5	1.05	14.1	32/31
$mPEG_{5k}$-PBG_{14}	11.2	1.05	6.7	13/–
$mPEG_{5k}$-PBG_{20}	12.6	1.06	7.2	17/–
$mPEG_{5k}$-PBG_{35}	17.5	1.07	9.1	32/–

[a] The molecular weight determined by ^{1}H NMR. [b] The degree of polymerization (DP) of PBG and PGA was calculated by ^{1}H NMR.

prepared and it was competent for acting as a macroinitiator for ROP of NCA.

The ^{1}H NMR spectra of $(mPEG_{5k})_2$-PBG_{35} and $(mPEG_{5k})_2$-PGA_{35} are collected in Fig. 4A and B, respectively. The peaks

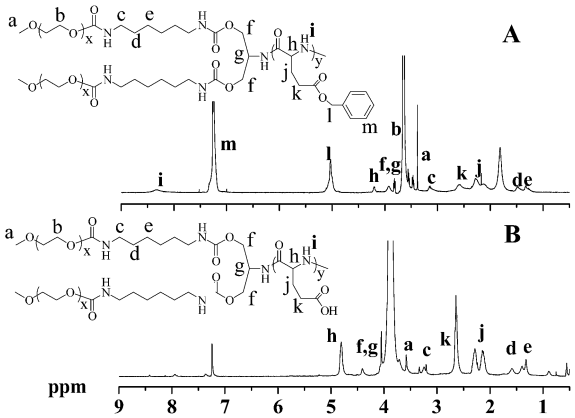

Fig. 4 ^{1}H NMR spectra of $(mPEG_{5k})_2$-PBG_{35}in $CDCl_3$ (A) and $(mPEG_{5k})_2$-PGA_{35} (B) in $CDCl_3$/CF_3COOD (v/v, 1 : 1).

marked with c, d and e are assigned to the protons of the hexamethylene group in HDI. The peaks i at 8.34 ppm, m at 7.25 ppm, l at 5.03 ppm, k at 2.62 ppm and j at 2.28 ppm are characteristic of the protons on the PBG main chain of $(mPEG_{5k})_2$-PBG_{35}. The peaks a and b are assigned to the protons of mPEG block of $(mPEG_{5k})_2$-PBG_{35}. The peaks f (4.18 ppm) and g (4.05 ppm) are assigned to the protons of $-(OCH_2)_2-CH-NH-$, $-(OCH_2)_2-CH-NH-$ units in serinol residue. For the preparation of $(mPEG_{5k})_2$-PGA_{35}, a solution of CF_3COOH and HBr 33 wt% in acetic acid was used as a deprotection reagent to remove the benzyl groups in $(mPEG_{5k})_2$-PBG_{35}. After deprotection, the peaks at 5.03 and 7.25 ppm assigned to the benzyl group in PBG disappeared almost completely in Fig. 4B, indicating complete removal of the protective groups.

The degree of polymerization (DP) of BLG in $(mPEG_{5k})_2$-PBG can be calculated by comparing the relative intensities of peak l and peak b in Fig. 4A. The DP of PGA in $(mPEG_{5k})_2$-PGA is calculated by a similar way. The DP data of PBG and PGA are listed in Table 1. It is clear that the DP of PBG of $(mPEG_{5k})_2$-PBG is well in accordance with feed composition, indicating almost complete conversion of BLG-NCA during the ROP of BLG-NCA. The little DP reduction of $(mPEG_{5k})_2$-PBG after deprotection demonstrates that CF_3COOH/HBr/acetic acid has no harmful effect on the degradation of the main chain of PBG segment of $(mPEG_{5k})_2$-PBG. Relatively, the molecular weight obtained by GPC is larger than that determined by ^{1}H NMR (Table 1), but Y-shaped copolymers shows low correction factor, and linear copolymer gives higher results. This result indicated the difference of various topologies.

The FT-IR spectra of $(mPEG_{5k})_2$-PBG_{35} and $(mPEG_{5k})_2$-PGA_{35} are shown in Fig. 2D and E. In comparison with that of $(mPEG_{5k})_2$-NH_2 in Fig. 2C, the peaks at 3297 cm^{-1}, 1651 cm^{-1} and 1549 cm^{-1} appeared and they are characteristic of NH stretching and amide I and amide II modes of PBG, respectively, indicating the formation of the polypeptide block. Moreover, the absorption peaks at 750 cm^{-1} and 700 cm^{-1} are attributed to the phenyl groups in the PBG block[23] The disappearance of these two peaks from Fig. 4E implies successful removal of the benzyl groups, and the red shift of the peak (C=O stretching)

from 1734 cm^{-1} to 1727 cm^{-1} and the blue shift of the peak (amide I mode) from 1651 cm^{-1} to 1655 cm^{-1} in Fig. 2E with respect to those in Fig. 2D can be ascribed to the enhanced hydrogen bonding between repeat units in PGA of $(mPEG_{5k})_2$-PGA_{35}.[24] The molecular weight of $(mPEG_{5k})_2$-PBG was characterized by GPC. As shown in Fig. 3 and Table 1, the GPC of $(mPEG_{5k})_2$-PBG_{20} (Curve D) showed even less retention time compared to that of $(mPEG_{5k})_2$-NHBoc (Curve C) and the Mw of $(mPEG_{5k})_2$-PBGs thus obtained were in the range of 12.7–15.5 kg mol^{-1}, indicating different hydrodynamic behaviors of them from that of linear PEG counterparts. Nevertheless, the PDIs of $(mPEG_{5k})_2$-PBGs calculated from GPC profiles were less than 1.08 (Table 1), indicating absence of side reactions and approximately living polymerization of BLG-NCA under the polymerization conditions employed. In conclusion, Y-shaped block copolymers $(mPEG_{5k})_2$-PBG and $(mPEG_{5k})_2$-PGA were successfully synthesized.

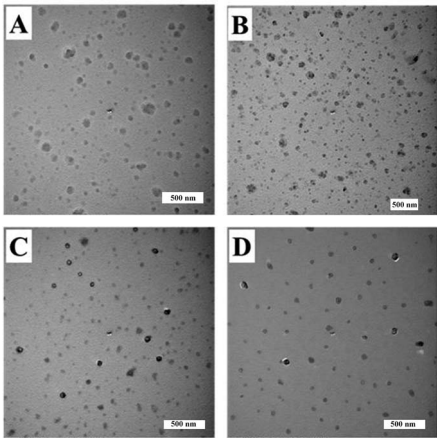

Fig. 5 TEM images of $(mPEG_{5k})_2$-PBG_{20} (A), $(mPEG_{5k})_2$-PBG_{35} (B), $mPEG_{5k}$-PBG_{20} (C), and $mPEG_{5k}$-PBG_{35} (D).

Self-assembly of copolymers in aqueous solution

A steady-state fluorescent spectroscopic method using pyrene as a probe was used to study self-assembly of linear and Y-shaped copolymers in aqueous solution. It is well known that the CMC values reflect the stability of micelles, *i.e.*, a low CMC value means a high stability of micelles.[25] It was reported that linear $mPEG_{20k}$-PBGs with the different molar ratio of PBG (14.9 to 4.8%) self-assembled into micelles in water, their CMC values ranged from 7.8 to 19.9 mg L^{-1}.[26] As listed in Table 2, the CMC values of $(mPEG_{5k})_2$-PBGs are in the range from 4.1 to 4.9 mg L^{-1}, close to those of $mPEG_{5k}$-PBGs, indicating that $(mPEG_{5k})_2$-PBGs can be a competent drug carrier.

$(mPEG_{5k})_2$-PBG consists of hydrophilic segments of $mPEG_{5k}$ and hydrophobic segment of PBG, and thus can self-assemble into micelles in aqueous solution, mPEG forms the outer shell while PBG forms the inner core. TEM and DLS were used to characterize the morphology and size of the micelles. As shown in Fig. 5, the micelles of both Y-shaped and linear mPEG-PBG show a spherical shape with a PDI value of 0.15–0.18, which shows a narrow distribution. As shown in Table 2, the sizes of $mPEG_{5k}$-PBG and $(mPEG_{5k})_2$-PBG both decrease with increasing length of hydrophobic PBG segment. The sizes of $(mPEG_{5k})_2$-PBG_{14}, $(mPEG_{5k})_2$-PBG_{20}, and $(mPEG_{5k})_2$-PBG_{35} determined by DLS are 123, 117, and 99 nm, respectively, higher than that of $mPEG_{5k}$-PBG_{14}, $mPEG_{5k}$-PBG_{20} and $mPEG_{5k}$-PBG_{35} (108, 87, and 88 nm), respectively. The possible reason is that at the same length of PBG, the molar ratio of mPEG/PBG in $(mPEG_{5k})_2$-PBG is two times that in $mPEG_{5k}$-PBG, resulting in a larger size of micelles. Comparatively, the size of $mPEG_{5k}$-PBG and $(mPEG_{5k})_2$-PBG determined by TEM is smaller than those determined by DLS because of the micelle shrinkage during TEM sample preparation. The size of $(mPEG_{5k})_2$-PBG ranges from 75 nm to 82 nm, and that of $mPEG_{5k}$-PBG is in the range from 60 to 62 nm. This is in agreement with DLS measurements.

Table 2 Parameters of linear and Y-shaped micelles

	Size (nm)		PDI	
Copolymers	by DLS	by TEM	by DLS	CMC (mg L^{-1})
$(mPEG_{5k})_2$-PBG_{14}	123	80	0.15	4.89
$(mPEG_{5k})_2$-PBG_{20}	117	82	0.16	4.55
$(mPEG_{5k})_2$-PBG_{35}	99	75	0.18	4.67
$mPEG_{5k}$-PBG_{14}	108	75	0.17	3.56
$mPEG_{5k}$-PBG_{20}	87	60	0.18	4.61
$mPEG_{5k}$-PBG_{35}	88	62	0.16	3.68

Synthesis and characterization of $(mPEG_{5k})_2$-PGA-PTX and $(mPEG_{5k})_2$-PGA–cisplain conjugates

Polymer prodrugs based on mPEG-PGA has been widely investigated and some of these polymer prodrugs have entered preclinical studies. These polymer prodrugs can enhance the solubility of hydrophobic drugs, such as paclitaxel, camptothecin, prolong the circulation time of loaded drugs, reduce system toxicity caused by anti-cancer small molecule drugs, and improve the quality of patients' lives.[27,28] In this work, for further exploring the potential of $(mPEG_{5k})_2$-PGA on the field of polymer prodrugs, Paclitaxel (PTX) and Cisplatin (Pt) were selected as model drugs and loaded into $(mPEG_{5k})_2$-PGA to prepare $(mPEG_{5k})_2$-PGA-PTX and $(mPEG_{5k})_2$-PGA-Pt conjugates, the *in vitro* and *in vivo* anti-cancer activities of them were further investigated.

Paclitaxel (PTX) is widely used in treatment of advanced and refractory ovarian, breast, lung, and head and neck cancers. Because of its low water solubility, it is usually administrated in the dose form of Taxol, *i.e.*, a suspension in Cremophor EL (a polyoxyethylene castor oil)/anhydrous ethanol (1 : 1) solution. Cremophor EL leads to severe side effects and lowers the antitumor efficacy of PTX.[29] In order to overcome these side effects, polymer–drug conjugates have been developed. For example, poly(L-glutamic acid)-paclitaxel conjugate (PGA-PTX, XYOTAX™, CT2103), now under phase III clinical trials, presents improved water solubility, self-assembles into ~80 nm

nanoparticles in aqueous solution, and shows enhanced anti-cancer activity and targeted accumulation at tumor site with the help of both cathepsin B and the enhanced permeability and retention (EPR) effect, which improve the efficacy of chemotherapy and reduce the side effects as compared to free Taxol.[30] Considering that PEG has merits of good water solubility, non-immunogenicity, chain mobility and long blood circulation time through prevention of renal elimination and avoidance of receptor-mediated protein uptake by cells of the reticuloendothelial system (RES),[31,32] PTX was conjugated to ($mPEG_{5k}$)-PGA_{35} for the preparation of $(mPEG)_2$-PGA-PTX conjugates. The structure, morphology, and *in vitro* anti-cancer efficacy of $mPEG_{5k}$-PGA-PTX were further investigated.

By virtue of the reactivity of hydroxyl groups in the 2′ position of PTX, it was conjugated onto $(mPEG_{5k})_2$-PGA_{35} with the help of DCC and DMAP to form an ester linkage.[33] The structure of $(mPEG_{5k})_2$-PGA_{35}-PTX was characterized by ^{1}H NMR. As shown in Fig. 6, the ^{1}H NMR spectrum (6A) of $(mPEG_{5k})_2$-PGA_{35}-PTX contains all feature peaks of PTX (6B) and $(mPEG_{5k})_2$-PGA_{35} (6C) except that of the proton (4.80 ppm) at the 2′ position of PTX, indicating successful synthesis of $(mPEG)_2$-PGA-PTX. The content of PTX in $(mPEG_{5k})_2$-PGA_{35}-PTX is about 20%, and the coupling efficiency of PTX was calculated to be 90% by using the relative integral areas of the protons of benzyl groups of PTX between 7.34 and 8.03 ppm with respect to that of the protons of –CH_2CH_2O– units of mPEG at 3.53 ppm. Similarly, $(mPEG)_2$-PGA-Pt conjugate was prepared by virtue the coordination of the carboxyl groups in PGA segment and the central Pt atom of cisplatin. The Pt content in the conjugate was determined by ICP-MS to be 15% (w/w).

$(mPEG_{5k})_2$-PGA_{35}-PTX and $(mPEG_{5k})_2$-PGA_{35}-Pt were allowed to self-assemble into nano-micelles (MPTX and MPt) in aqueous solution. TEM micrographs in Fig. 7A and B revealed the spherical shape of the micelles formed. The average particle size was about 50 nm for MPTX and about 45 nm for MPt. It implies that although PGA is hydrophilic to some extent, the conjugate PGA_{35}-PTX or PGA_{35}-Pt as a whole is indeed hydrophobic. Therefore, the mPEG segments forms the outer shell and the hydrophobic PGA-PTX or PGA-Pt segment forms the core of micelles. To confirm this structure, the frozen-dried MPTX micelles were re-dissolved in D_2O for ^{1}H NMR measurement. As shown in Fig. 7C, the peak at 3.64 ppm assigned to the protons of –CH_2CH_2O– units remained, while the characteristic signals associated with the PGA-PTX segment were all absent.

The cytotoxicity of MPTX, and MPt against MCF-7, HeLa and SMMC cell lines was evaluated by MTT assay in comparison with that of $(mPEG)_2$-PGA_{35}, PTX, and Pt. As shown in Fig. 8, the cell viability of $(mPEG_{5k})_2$-PGA_{35} treated cells was higher than 90% no matter at 48 or 72 h, indicating very low toxicity of $(mPEG)_2$-PGA as a drug carrier material. As shown in Fig. 9, the

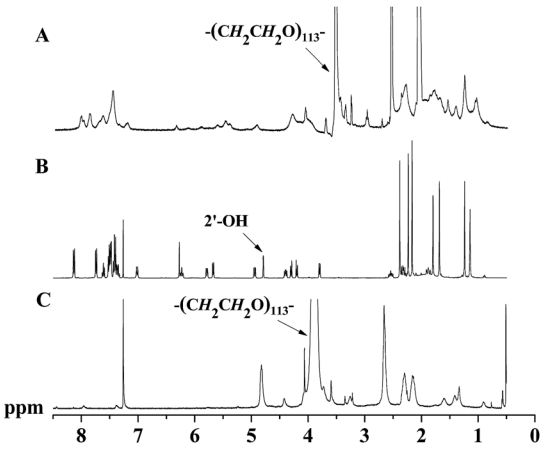

Fig. 6 ^{1}H NMR spectra of $(mPEG_{5k})_2$-PGA_{35}-PTX (A) in DMSO/CF_3-COOD (v/v, 1 : 1), PTX in $CDCl_3$ (B) and $(mPEG_{5k})_2$-PGA_{35} (C) in $CDCl_3$/CF_3COOD (v/v, 1 : 1).

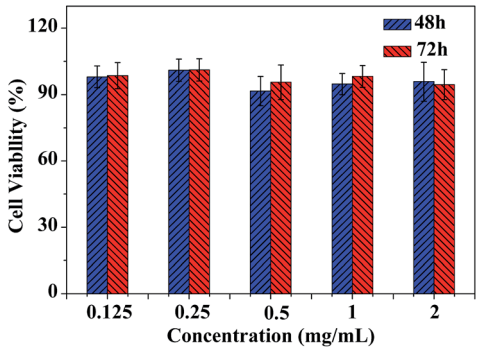

Fig. 8 *In vitro* cytotoxicity of $(mPEG_{5k})_2$-PGA_{35} for 48 h and 72 h against MCF-7 cell line.

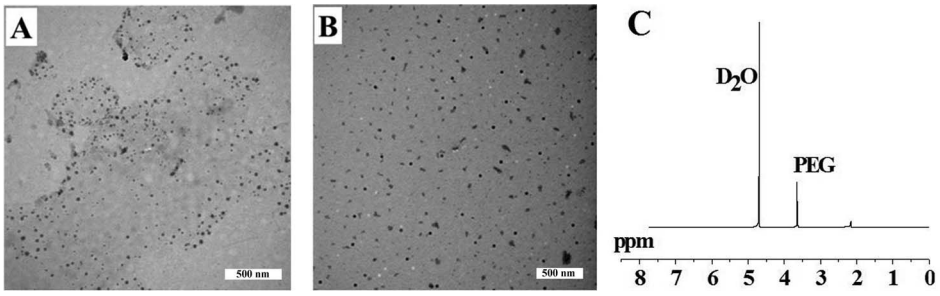

Fig. 7 TEM images of $(mPEG_{5k})_2$-PGA_{35}-PTX (A) and $(mPEG_{5k})_2$-PGA_{35}-Pt (B) particles. (C) ^{1}H NMR spectrum of frozen-dried $(mPEG_{5k})_2$-PGA_{35}-PTX micelles in D_2O.

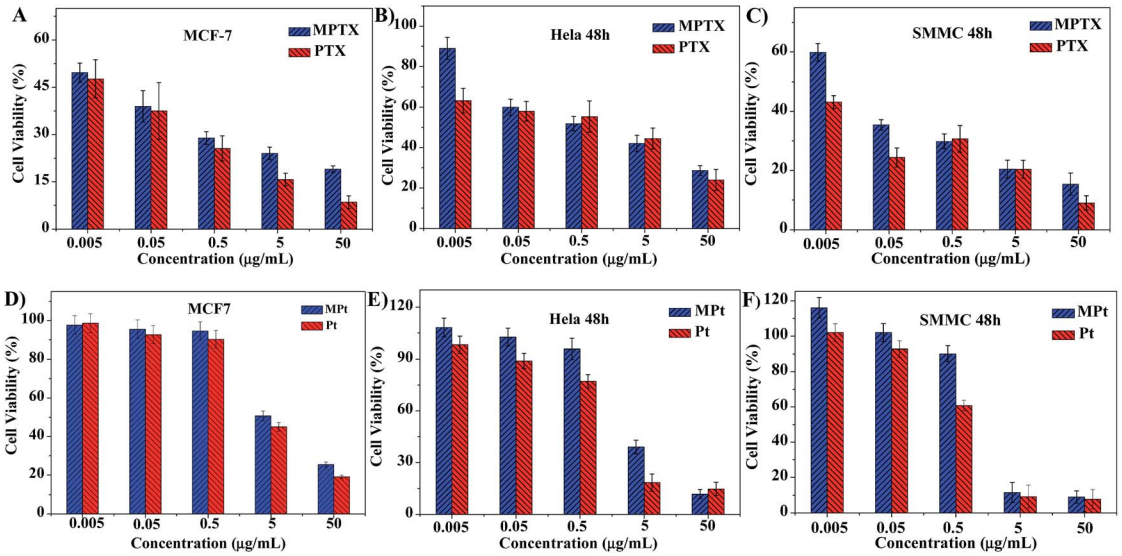

Fig. 9 MTT assay results at 48 h: (A) MPTX and PTX for MCF7; (B)MPTX and PTX for HeLa; (C) PTX and PTX for SMMC; (D) Pt and cisplatin for MCF7; (E) Pt and cisplatin for HeLa; (F) MPt and Pt for SMMC.

cell viability showed obvious concentration dependence and cell line dependence for PTX, MPTX, Pt, and MPt. Based on the concentration dependence, IC_{50} was calculated and collected in Table 3. Firstly, given a formulation, IC_{50} of MPTX varied from less than 0.005 μg ml^{-1} for MCF-7 to 1.24 μg ml^{-1} for HeLa cells, approximately corresponding to that of pure PTX; while IC_{50} of MPt varied from 9.11 μg ml^{-1} for MCF-7 to 1.76 μg ml^{-1} for SMMC cells, approximately in parallel to that of pure Pt. This is understandable, because every anti-cancer drug is not effective to all cancers. Secondly, for each cell line tested, MPTX and MPt displayed comparable or a little bit less cytotoxicity than pure PTX and Pt, respectively. Because MPTX and MPt as nano-micelles have other advantages over PTX and Pt, *e.g.*, reduced systemic toxicity, this comparable cytotoxicity implies possibility for them to be used as effective drug delivery systems.

In vivo antitumor activity of MPt

Cisplatin (abbr. as Pt) is a first line anti-cancer drug for treatment of many malignancies, such as ovarian, bladder, non-small-cell lung and liver cancers. H22 is a well-known cell line obtained from human liver carcinoma. In this work, H22 bearing Kunming mice were treated i.v. three times at 2 day intervals at the same dose of 3 mg and 6 mg Pt per kg for cisplatin and MPt. The relative tumor volume (RTV) *vs.* time and the relative body weight *vs.* time are shown in Fig. 10. As shown in Fig. 10A, the RTV increment of four groups took an order of Saline ≫ MPt (3 mg Pt per kg^{-1}) > Pt (3 mg Pt per kg) > MPt (6 mg Pt per kg). For example, on the 14th day, the RTV values were 343.9 ± 25.2, 81.5 ± 10.7, 34.7 ± 8.0, and 16.9 ± 3.8, respectively. Notably, increasing the dose of MPt from 3 mg Pt

Table 3 IC_{50} values of MPTX, PTX, MPt, and Pt against MCF7, HeLa, and SMMC cell lines

	IC_{50} (μg ml^{-1})		
Drugs	MCF7	HeLa	SMMC
MPTX	<0.005	1.24	0.01
PTX	<0.005	0.34	<0.005
MPt	9.11	4.58	1.76
Pt	5.28	1.42	1.34

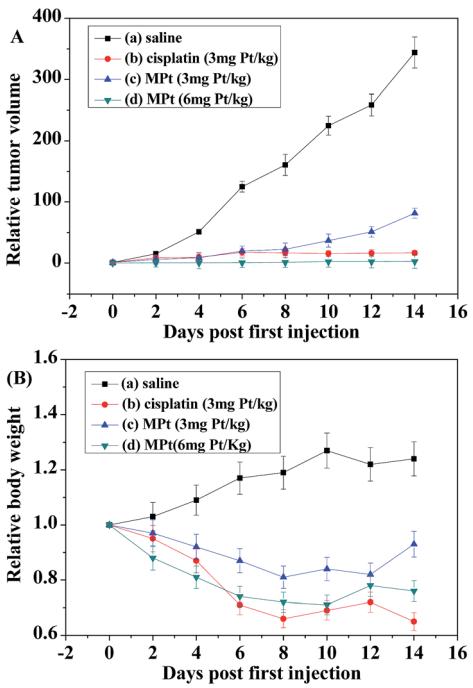

Fig. 10 Relative tumor volume (A) and relative body weight (B) of the H22 cancer bearing mice as a function of time. (a) saline; (b) cisplatin (3 mg Pt per kg); (c) MPt (3 mg Pt per kg); (d) MPt (6 mg Pt per kg).

per kg to 6 mg Pt per kg led to enhanced anti-cancer efficacy while similar increase in cisplatin dose caused death of all test mice on the 4th day post first injection, indicating the lower systemic toxicity of MPt than cisplatin. This conclusion was supported by the body weight measurement. As shown in Fig. 10B, the relative body weight took an order of Saline ≫ MPt (3 mg Pt per kg) > MPt (6 mg Pt per kg) > Pt (3 mg Pt per kg) on day 14.

Conclusions

A novel strategy for preparing Y-shaped amphiphilic $(mPEG)_2$-PBG copolymer containing two hydrophilic arms and one hydrophobic arm was successfully developed, that is, to prepare $(mPEG)_2$-PBG by using a macroinitiator with a middle primary amino group $(mPEG)_2$-NH_2 to initiate the ROP of γ-benzyl-L-glutamate-*N*-carboxyanhydride. Due to its amphiphilic nature, $(mPEG)_2$-PBG can self-assemble into micelles and can encapsulate hydrophobic drugs. After removal of the benzyl groups on the PBG segment, the copolymer became $(mPEG)_2$-PGA containing free carboxyl groups. By virtue of these carboxyl groups, $(mPEG)_2$-PGA could conjugate with hydrophobic drugs like PTX and Cisplatin. The conjugates formed were also amphiphilic and were allowed to self-assemble into nanoscale drug formulations, which showed good water solubility, satisfactory cytotoxicity to cancer cells and excellent antitumor efficacy to H22 cancers. Therefore, polymer nano-prodrug based on $(mPEG)_2$-PGA has a potential in the treatment of solid-tumors.

Acknowledgements

Financial support was provided by the National Science Foundation of China (Project no. 51003101, 91227118, and 51373167).

Notes and references

1 R. Gref, M. Lück, P. Quellec, M. Marchand, E. Dellacherie, S. Harnisch, T. Blunk and R. H. Müller, *Colloids Surf., B*, 2000, **18**, 301–313.
2 W. Chen, F. H. Meng, F. Li, S.-J. Ji and Z. Y. Zhong, *Biomacromolecules*, 2009, **10**, 1727–1735.
3 Y. Bae and K. Kataoka, *Adv. Drug Delivery Rev.*, 2009, **61**, 768–784.
4 K. Cho, X. Wang, S. Nie, Z. G. Chen and D. M. Shin, *Clin. Cancer Res.*, 2008, **14**, 1310–1316.
5 H. Maeda, J. Wu, T. Sawa, Y. Matsumura and K. Hori, *J. Controlled Release*, 2000, **65**, 271–284.
6 J. Khandare and T. Minko, *Prog. Polym. Sci.*, 2006, **31**, 359–397.
7 J. X. Ding, C. S. Xiao, L. Zhao, Y. L. Cheng, L. L. Ma, Z. H. Tang, X. L. Zhuang and X. S. Chen, *J. Polym. Sci., Part A: Polym. Chem.*, 2011, **49**, 2665–2676.
8 L. Y. Qiu and Y. H. Bae, *Pharm. Res.*, 2006, **23**, 1–30.
9 G. Lapienis, *Prog. Polym. Sci.*, 2009, **34**, 852–892.
10 C. Garofalo, G. Capuano, R. Sottile, R. Tallerico, R. Adami, E. Reverchon, E. Carbone, L. Izzo and D. Pappalardo, *Biomacromolecules*, 2014, **15**, 403–415.
11 J. Sun, X. S. Chen, J. S. Guo, Q. Shi, Z. G. Xie and X. B. Jing, *Polymer*, 2009, **50**, 455–461.
12 H. Cabral, M. Murakami, H. Hojo, Y. Terada, M. R. Kano, U. I. Chung, N. Nishiyama and K. Kataoka, *Proc. Natl. Acad. Sci. U. S. A.*, 2013, **110**, 11397–11402.
13 M. Yokoyama, T. Okano, Y. Sakurai, S. Suwa and K. Kataoka, *J. Controlled Release*, 1996, **39**, 351–356.
14 H. Cabral, N. Nishiyama and K. Kataoka, *J. Controlled Release*, 2007, **121**, 146–155.
15 J. Schulz, H. Burris, C. Redfern, M. Warner and C. Paradise, *Eur. J. Cancer*, 2002, **38**, S132.
16 Y. Matsumura and K. Kataoka, *Cancer Sci.*, 2009, **100**, 572–579.
17 J. X. Ding, C. L. He, C. S. Xiao, J. Chen, X. L. Zhuang and X. S. Chen, *Macromol. Res.*, 2012, **20**, 292–301.
18 C. Neri and J. M. J. Williams, *Adv. Synth. Catal.*, 2003, **345**, 835–848.
19 L. X. Yang, H. H. Xiao, L. S. Yan, R. Wang, Y. B. Huang, Z. G. Xie and X. B. Jing, *J. Mater. Chem. B*, 2014, **2**, 2097.
20 L. X. Yang, J. Z. Wei, L. S. Yan, Y. B. Huang and X. B. Jing, *Biomacromolecules*, 2011, **12**, 2032–2038.
21 L. S. Yan, L. X. Yang, H. Y. He, X. L. Hu, Z. G. Xie, Y. B. Huang and X. B. Jing, *Polym. Chem.*, 2012, **3**, 1300–1307.
22 L. S. Yan, W. B. Wu, W. Zhao, R. G. Qi, D. M. Cui, Z. G. Xie, Y. B. Huang, T. Tong and X. Jing, *Polym. Chem.*, 2012, **3**, 2403–2413.
23 J. Yue, R. Wang, S. Liu, S. H. Wu, Z. G. Xie, Y. B. Huang and X. B. Jing, *Soft Matter*, 2012, **8**, 7426–7435.
24 C. Deng, G. Z. Rong, H. Y. Tian, Z. H. Tang, X. S. Chen and X. B. Jing, *Polymer*, 2005, **46**, 653–659.
25 C. Agatemor and M. P. Shaver, *Biomacromolecules*, 2013, **14**, 699–708.
26 Y. I. Jeong, J. W. Nah, H. C. Lee, S. H. Kim and C. S. Cho, *Int. J. Pharm.*, 1999, **188**, 49–58.
27 H. H. Xiao, R. G. Qi, S. Liu, X. L. Hu, T. C. Duan, Y. H. Zheng, Y. B. Huang and X. B. Jing, *Biomaterials*, 2011, **32**, 7732–7739.
28 X. L. Hu, S. Liu, Y. B. Huang, X. S. Chen and X. B. Jing, *Biomacromolecules*, 2010, **11**, 2094–2102.
29 L. Sheihet, O. B. Garbuzenko, J. Bushman, M. K. Gounder, T. Minko and J. Kohn, *Eur. J. Pharm. Sci.*, 2012, **45**, 320–329.
30 J. Gligorov and J. P. Lotz, *Oncologist*, 2004, **9**(suppl. 2), 3–8.
31 J. P. Nam, J. K. Park, D. H. Son, T. H. Kim, S. J. Park, S. C. Park, C. Choi, M. K. Jang and J. W. Nah, *Colloids Surf., B*, 2014, **120**, 168–175.
32 H. Otsuka, Y. Nagasaki and K. Kataoka, *Adv. Drug Delivery Rev.*, 2003, **55**, 403–419.
33 C. Li, D. F. Yu, R. A. Newman, F. Cabral, L. C. Stephens, N. Hunter, L. Milas and S. Wallace, *Cancer Res.*, 1998, **58**, 2404–2409.

